

Fermi National Accelerator Laboratory

FERMILAB-Conf-99/020-E

KTeV/E832

The Measurement of ϵ'/ϵ at Fermilab KTeV-E832

Yee Bob Hsiung

*Fermi National Accelerator Laboratory
P.O. Box 500, Batavia, Illinois 60510*

February 1999

Published Proceedings of the *International Workshop on CP Violation in K*,
KEK Tanashi Branch, Tanashi, Tokyo, Japan, December 18-19, 1998

Disclaimer

This report was prepared as an account of work sponsored by an agency of the United States Government. Neither the United States Government nor any agency thereof, nor any of their employees, makes any warranty, expressed or implied, or assumes any legal liability or responsibility for the accuracy, completeness, or usefulness of any information, apparatus, product, or process disclosed, or represents that its use would not infringe privately owned rights. Reference herein to any specific commercial product, process, or service by trade name, trademark, manufacturer, or otherwise, does not necessarily constitute or imply its endorsement, recommendation, or favoring by the United States Government or any agency thereof. The views and opinions of authors expressed herein do not necessarily state or reflect those of the United States Government or any agency thereof.

Distribution

Approved for public release; further dissemination unlimited.

Copyright Notification

This manuscript has been authored by Universities Research Association, Inc. under contract No. DE-AC02-76CHO3000 with the U.S. Department of Energy. The United States Government and the publisher, by accepting the article for publication, acknowledges that the United States Government retains a nonexclusive, paid-up, irrevocable, worldwide license to publish or reproduce the published form of this manuscript, or allow others to do so, for United States Government Purposes.

The measurement of ϵ'/ϵ at Fermilab KTeV-E832

Yee Bob Hsiung*

*Fermi National Accelerator Laboratory
P.O. Box 500, Batavia, Illinois, USA*

(KTeV Collaboration: Arizona, Chicago, Colorado,
Elmhurst, Fermilab, Osaka, Rice, Rutgers,
UCLA, UCSD, Virginia and Wisconsin)

Abstract

The status of the analysis effort for the 25% data sample taken during the Fermilab '96-'97 fixed target run for ϵ'/ϵ measurement from KTeV is presented here. Detector performance, data statistics, background subtractions, data and monte-carlo comparison for acceptance corrections, as well as the preliminary results on $K_L \rightarrow \pi^0 \gamma \gamma$ are described in more detail. Prospects for KTeV99, in the up coming 6-months '99 fixed target run, are also discussed here.

*electronic address: hsiung@fnal.gov

1 Introduction

One of the best established methods for studying the origin of CP violation rests in the observation of both K_L and K_S decays into $\pi^+\pi^-$ and $2\pi^0$ [1][2][3]. If the CKM matrix is indeed the source of CP violation, the parameter ϵ'/ϵ , derived from the double ratio of these decays, is expected to be non-zero[4].

Experimentally we would measure the double ratio R ,

$$R = \frac{\Gamma(K_L \rightarrow \pi^+\pi^-)/\Gamma(K_S \rightarrow \pi^+\pi^-)}{\Gamma(K_L \rightarrow \pi^0\pi^0)/\Gamma(K_S \rightarrow \pi^0\pi^0)} \approx 1 + 6\text{Re}(\epsilon'/\epsilon). \quad (1)$$

The two most recent results from Fermilab-E731[2] and CERN-NA31[3] were

$$\text{Re}(\epsilon'/\epsilon) = (7.4 \pm 5.2(\text{stat}) \pm 2.9(\text{syst})) \times 10^{-4}, \quad (E731) \quad (2)$$

$$\text{Re}(\epsilon'/\epsilon) = (2.3 \pm 3.5(\text{stat}) \pm 5.5(\text{syst})) \times 10^{-4}. \quad (NA31) \quad (3)$$

which gave inconclusive interpretations between Standard Model CP-violation[5][6] and Superweak CP-violation[7] at a precision of 7×10^{-4} total error with a statistics sample of $\sim 400k$ $K_L \rightarrow 2\pi^0$ events collected in these experiments (the limiting statistics channel of the four decay modes in the double ratio, as shown in Eq. 1).

With the capability of producing high flux neutral kaon beam, large yield, low background, the new experiments such as Fermilab-KTeV, CERN-NA48[8] and DAPHNI-KLOE[9] (with large acceptance and long decay region, precision detection technology, high-speed electronics and data acquisition system with low deadtime), can now collect millions of good 2π decays toward the goal of 10^{-4} precision measurement of $\text{Re}(\epsilon'/\epsilon)$. Such measurements are likely to be the first ones to establish the “direct” CP-violating effect before B-factory experiments and other rare K and B decays[10].

2 KTeV Detector and Performance

The KTeV apparatus is shown in Figure 1. Two side-by-side neutral kaon beams were produced by 800 GeV protons striking a 30 cm long BeO target and a series of precision collimators and sweeping magnets. Typical primary intensity was 3×10^{12} per spill. Each spill was 20 sec long and came in every 60 sec. About 100 meters downstream of target of the experiment (followed by 58 meters long vacuum decay region) the kaon component of these beams was predominately K_L . The K_S was produced by regeneration of K_L striking a regenerator placed in one of the beams. The regenerator was moved from one beam to the other every beam spill to reduce systematics due to beam and detector asymmetries. The regenerator, about 1.7 meters long, was made of a fully active blocks of scintillators to reject backgrounds from inelastic scattering and interactions. Only coherently regenerated K_S decays were used for ϵ'/ϵ measurement.

The momenta of charged particles from the decay were measured with four drift chambers, two on each side of an analysis magnet with 400 MeV/c kick in transverse momentum. Each chamber consisted of four wire planes in two orthogonal views (x, x' and y, y').

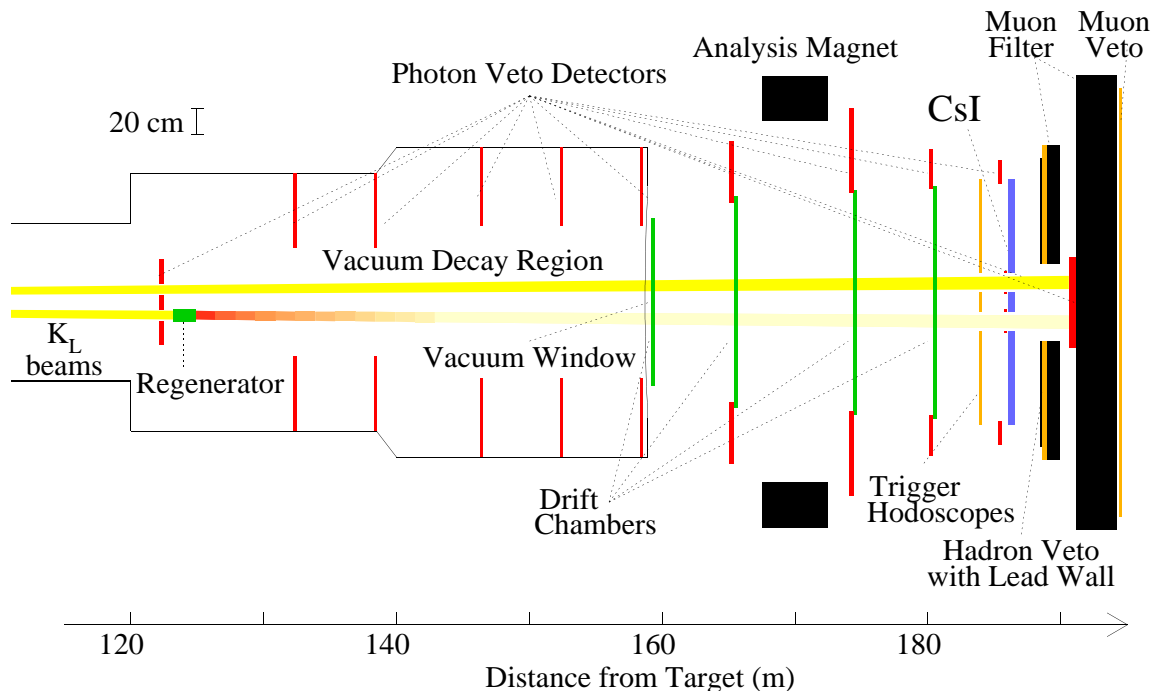


Figure 1: Plan view of KTeV detector (E832 e'/e configuration).

About 100 micron resolution was achieved for each plane. To improve the resolution, gold-plated aluminum cathode wires were used in the chambers, and helium bags were placed between chambers to reduce the multiple scattering in the spectrometer for the charged particles. A CsI electromagnetic calorimeter[11] is used to measure the position and energy of photons and electrons from the decay. Total 3100 CsI crystals were arranged in a $1.9\text{ m} \times 1.9\text{ m}$ square array located 186 meters from target. A typical online event display of a $K \rightarrow 2\pi^0$ decay is shown in Figure 2. The central part of CsI array consisted 2232 small crystals ($2.5\text{ cm} \times 2.5\text{ cm}$), the outer part are large crystals ($5.0\text{ cm} \times 5.0\text{ cm}$). Each crystal is 50 cm long, about 27 radiation lengths. A nearly hermetic photon veto system (up to 100 mrad) was used to veto events in which one or more photons escape the detector. The typical veto threshold for online trigger was about $500\text{ MeV}/c^2$ in the photon veto system. The veto threshold for regenerator was 0.7 mips (minimum ionizing particle equivalent) for the last scintillator module and about 2 mips for the others. A set of trigger hodoscopes just upstream of CsI calorimeter is used to trigger on charged decay modes. Both CsI and trigger hodoscopes have two beam holes to allow the high intensity neutral beam to pass through. Muons were vetoed by a scintillator hodoscope after 3 meters of iron shielding behind CsI calorimeter. CsI calorimeter was calibrated online with K_{e3} electrons throughout the run. Better than 2% stability was maintained during the data taking with about 1% online resolution. Drift chamber was also calibrated online with semileptonic two-track events. A level-3 software filter reconstruction was used to make further reduction in the trigger.

Figure 3 shows the average energy resolution of the CsI from a sample of 190 million

calibration K_{e3} electrons of the first 25% data sample. The clustering algorithm for the energy and position of an electromagnetic shower in CsI calorimeter is based on 7×7 blocks for small crystals and 3×3 blocks for large crystals centered on the crystal with peak energy, as shown in Figure 2. We obtained 0.75% resolution on E/p for electrons in this sample, as shown in Figure 3(a). The linearity is better than 0.1% and the corresponding intrinsic energy resolution for photon is less than 1% at 4 GeV and better than 0.6% for the photon energy above 20 GeV, as shown in Figure 3(b). The position resolution is about 1 mm. The resulting mass resolution for $\pi^0\pi^0$ is 1.6 MeV/c² and 1.8 MeV/c² for $\pi^+\pi^-$ in the magnetic spectrometer.

Table 1 shows the improvements and comparisons of various beam and detector parameters from the KTeV experiment with the performance of previous E731/E773/E799-I experiments at Fermilab, which used a lead-glass calorimeter and similar drift chamber spectrometer[2].

Parameter	E731/E773/E799	KTeV
Pressure in decay region	500 μ Torr	1 μ Torr
μ flux per proton on target	4×10^{-5}	2×10^{-7}
Max. proton flux/spill	2.0E12	5.0E12
Calorimeter radiation exposure (E799)	450 rad/E12/week	50 rad/E12/week
γ energy resolution at 20 GeV/c	3.5%	0.65%
calorimeter nonlinearity (3-75 GeV/c)	10%	0.4%
π/e rejection, calorimeter	~ 50	~ 400
Magnetic field (p_t kick)	200 MeV/c	400 MeV/c
Magnetic field nonuniformity	5%	1%
Material in spectrometer (rl)	$\sim 0.87\%$	$\sim 0.35\%$
Single wire plane resolution	$\sim 85\mu\text{m}$	$\sim 100\mu\text{m}$
Track momentum resolution at 20 GeV/c	0.5%	0.25%
2μ efficiency	82%	99%
Regenerator: Inelastic background in vac. beam	$\sim 1.8\%$	$\sim 0.3\%$
γ veto performance (p.e. / MeV)	0.02	0.2
π/e rejection, TRD system	NA	~ 150
Level 2 clustering-trigger time	30 μs	2 μs
Level 2 tracking-trigger time	3 μs	1.5 μs
Level 2 TRD-trigger time	NA	1 μs
Level 3 complete event reconstruction	NA	200k events/spill
DAQ output	~ 20 MB / spill	~ 300 MB/spill
Livetime	0.7 at 0.8E11 p/spill	0.7 at 3.5E12 p/spill
Offline $\pi^0\pi^0$ mass resolution (MeV/c ²)	5.5	1.6
Offline $\pi^+\pi^-$ mass resolution (MeV/c ²)	3.5	1.8

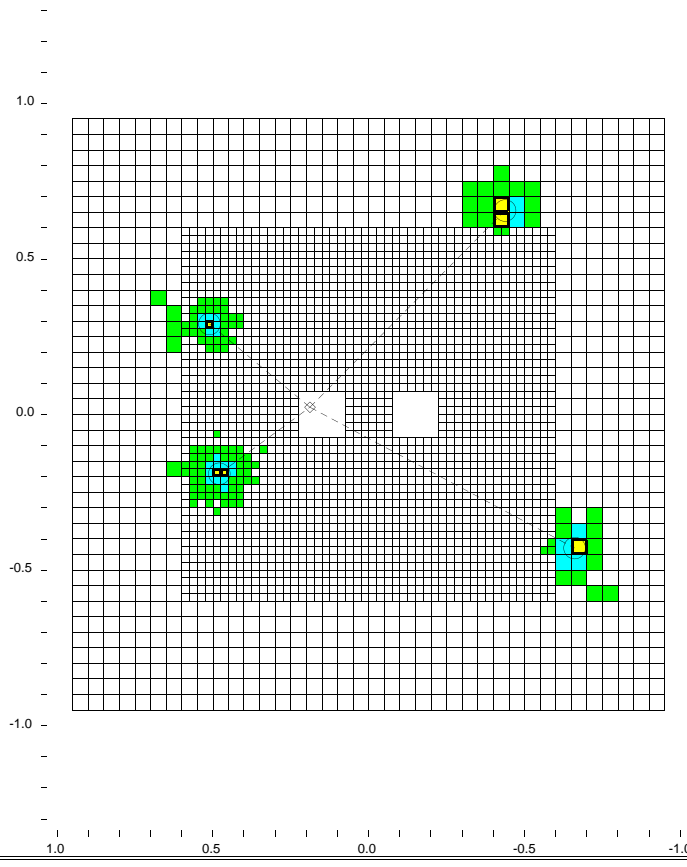
Table 1: Comparison between E731/E773/E799 and KTeV.

KTEV Event Display
 /ktev4a/data/E832/RAN009686.dat

Run Number: 9686
 Spill Number: 3
 Event Number: 534355
 Trigger Mask: 8
 All Slices

Track and Cluster Info
 HCC cluster count: 4
 ID Xcsi Ycsi P or E
 C 1: -0.4372 0.6553 6.20
 C 2: -0.6604 -0.4297 5.32
 C 3: 0.4797 -0.1908 18.65
 C 4: 0.5111 0.2909 9.24

Vertex: 4 clusters
 X Y Z
 0.1412 0.0171 139.139
 Mass=0.4973
 Pairing chisq=0.11



- - Cluster
- - Track
- - 10.00 GeV
- - 1.00 GeV
- - 0.10 GeV
- - 0.01 GeV

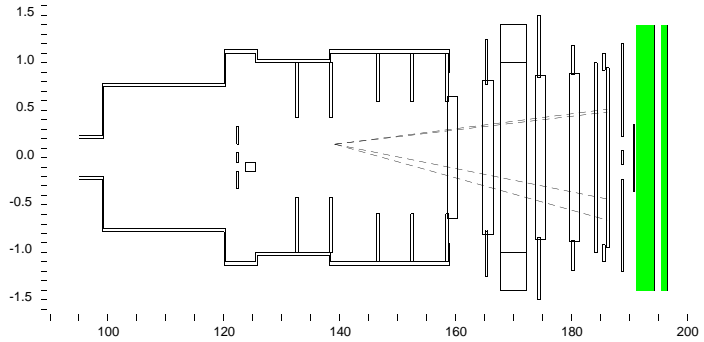


Figure 2: A typical online event display of a $K \rightarrow 2\pi^0$ decay.

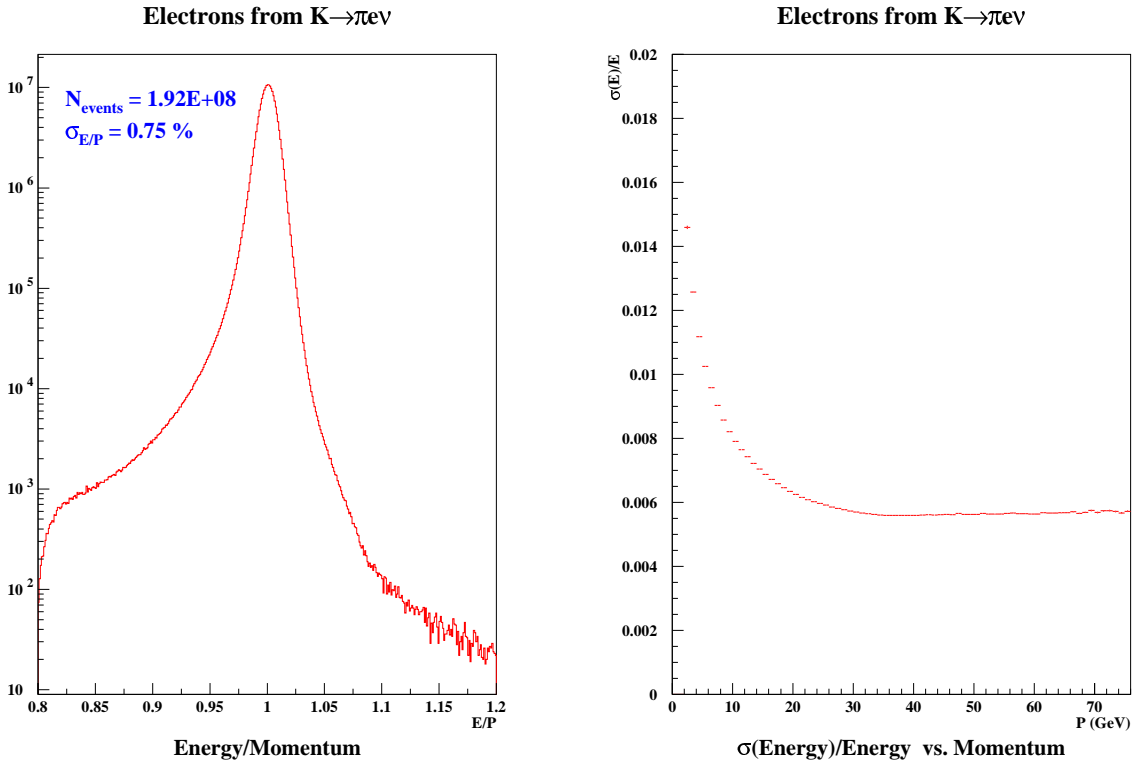


Figure 3: (a) Measured E/p (calorimeter energy / spectrometer momentum) for a sample of calibration electrons from $K_L \rightarrow \pi^\pm e^\mp \nu$ events; (b) Intrinsic $\sigma(E/p)$ versus momentum for these electrons after subtracting the contribution of tracking resolution.

3 Status of ϵ'/ϵ Analysis

The ϵ'/ϵ data were taken during '96 and '97 fixed target run at Fermilab. About 4 million $K_L \rightarrow 2\pi^0$ events after offline cuts (the limiting statistics mode) were collected during this running period. The analysis is currently concentrated on about 25% data sample, which includes $\pi^0\pi^0$ data from 7 weeks running at the end of 1996 and $\pi^+\pi^-$ data from first 18-days of running in 1997. The 1996 $\pi^+\pi^-$ data were not used in the current analysis due to a drift chamber pathology (lower gas gain and higher threshold relative to the first avalanche pulse in the chamber) combined with level-3 software cut caused a 20% loss in the trigger and a possible systematics of 0.5% in the single ratio of K_L/K_S for charged $\pi^+\pi^-$ decays. This effect has been quickly discovered during the run and corrected in the level-3 trigger for 1997 data.

The preliminary statistics of this data set for all four modes is shown below in Table 2 with the background fraction determined by the background subtraction described below.

ϵ'/ϵ mode	Preliminary data statistics	Total background fraction
Vac($K_L \rightarrow \pi^0\pi^0$)	1.0×10^6	0.72%
Reg($K_S \rightarrow \pi^0\pi^0$)	1.6×10^6	1.37%
Vac($K_L \rightarrow \pi^+\pi^-$)	1.9×10^6	0.08%
Reg($K_S \rightarrow \pi^+\pi^-$)	3.9×10^6	0.09%

Table 2: Statistics and background fraction of ϵ'/ϵ analysis for 25% data sample.

Figure 4 shows the various background contributions in the square of transverse momentum (p_t^2) distribution for $K_L \rightarrow \pi^+\pi^-$ and $K_S \rightarrow \pi^+\pi^-$ events. The background in K_S is dominated by the remaining regenerator scattering events not rejected by the 0.7 *mips* regenerator veto cut. The background in K_L is dominated by the remaining mis-identified semileptonic decays from the CsI calorimeter and muon veto system. Both backgrounds in charged mode are quite small, less than 0.1% for the events underneath the signal region with $488 < m_{\pi^+\pi^-} < 508 \text{ MeV}/c^2$ and $p_t^2 < 0.00025 \text{ GeV}^2/c^2$, and can be simulated well by Monte Carlo.

In the $\pi^0\pi^0$ neutral mode, the dominate backgrounds is from the remaining regenerator scattering which is shown in Figure 5 for both K_L and K_S decays. Same monte-carlo simulation for the regenerator scattering as in charged $\pi^+\pi^-$ mode was used to normalize the scattered background in the center of energy equal-area box-ring distributions for $\pi^0\pi^0$ mode. Scattering from the lips of last defining-collimator at 85 meters was also included in the simulation as shown in both Figure 4 and 5. The background was estimated with a cut at 110 in the box-ring number plot. The $3\pi^0$ background contribution underneath the $\pi^0\pi^0$ mass peak ($488 < m_{\pi^+\pi^-} < 508 \text{ MeV}/c^2$) is quite small comparing with previous E731 experiment, about 0.26% for K_L and 0.01% for K_S , as shown in Figure 6. The improvement is due to the nearly hermetic photon veto system (with an offline veto thresholds at $300 \text{ MeV}/c^2$) and fantastic resolution of CsI calorimeter.

A blind analysis approach has been used for the systematic study of the ϵ'/ϵ measure-

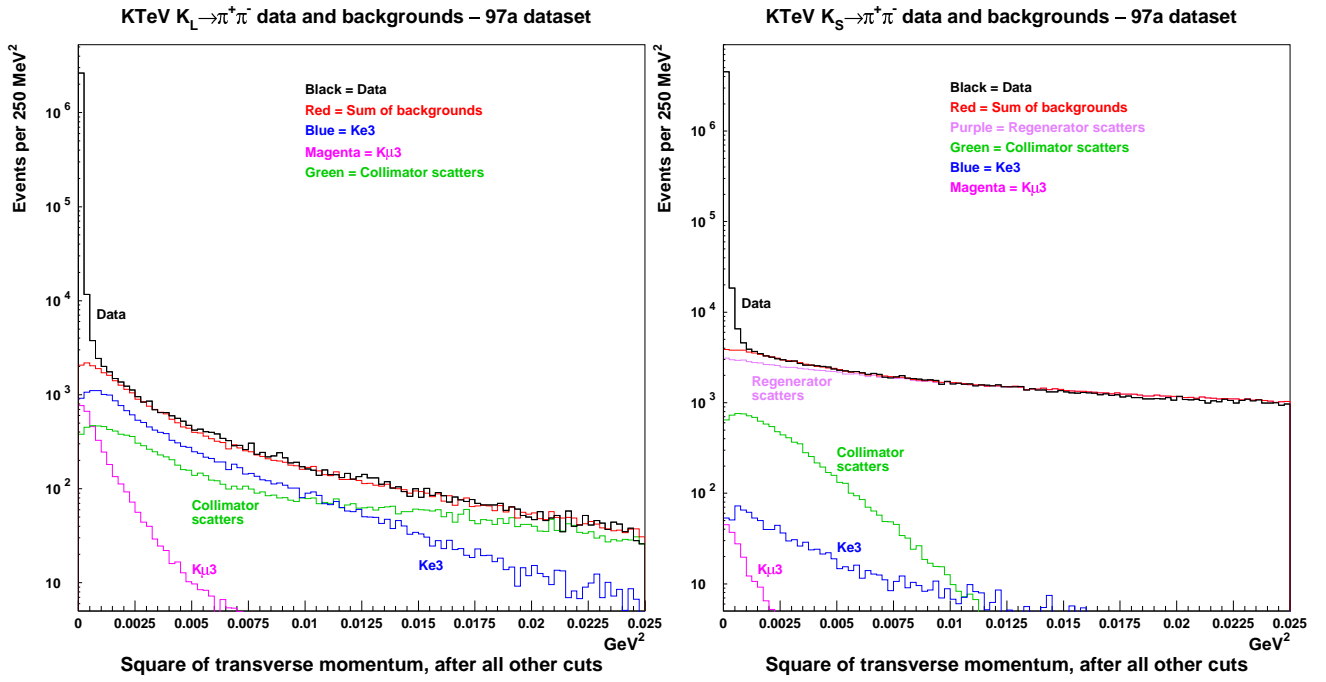


Figure 4: The square of transverse momentum (p_t^2) distribution for (a) $K_L \rightarrow \pi^+ \pi^-$ and (b) $K_S \rightarrow \pi^+ \pi^-$ events after all other cuts. Various background contributions from remaining semileptonic decays and regenerator scattering are also shown here.

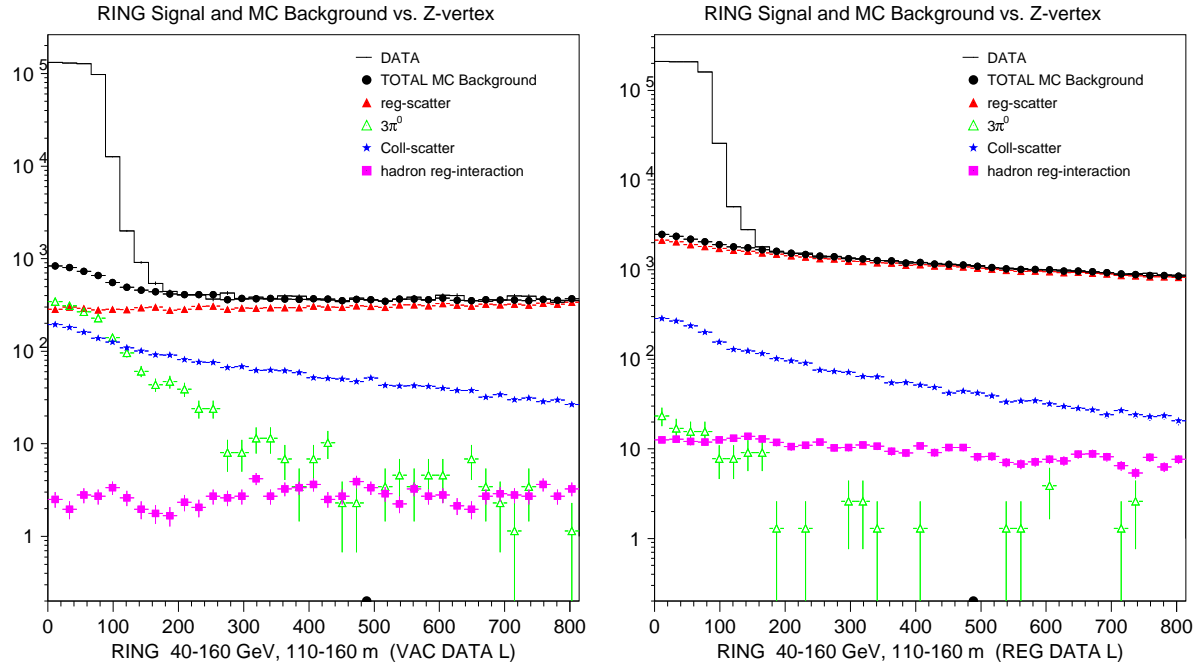


Figure 5: The center of energy box-ring distributions for (a) $K_L \rightarrow \pi^0\pi^0$ and (b) $K_S \rightarrow \pi^0\pi^0$ events after all other cuts. Various background contributions from remaining regenerator scattering, defining-collimator scattering and $3\pi^0$ background are also shown here.

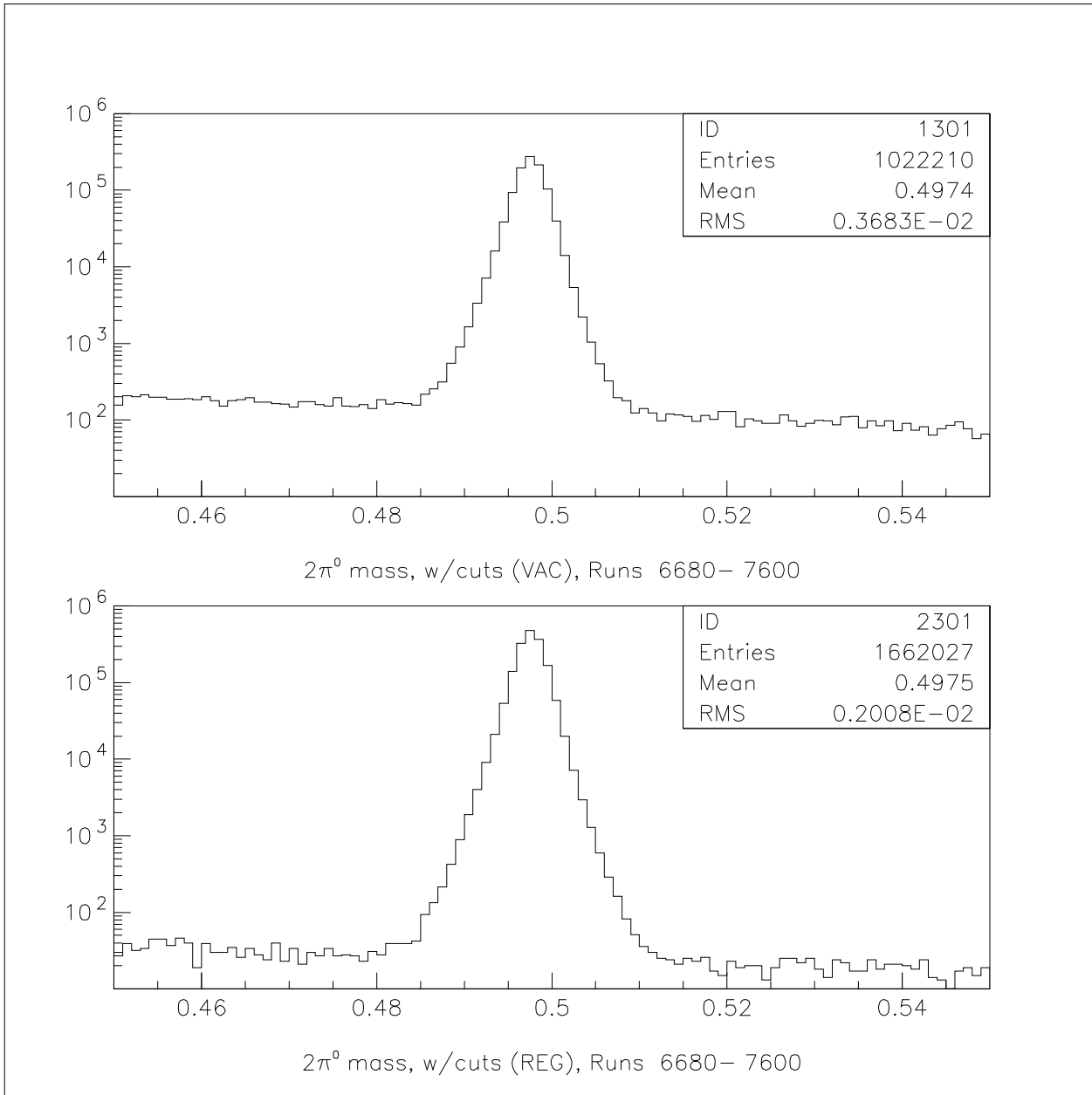


Figure 6: $\pi^0\pi^0$ mass distributions for (a) $K_L \rightarrow \pi^0\pi^0$ and (b) $K_S \rightarrow \pi^0\pi^0$ events, after all other cuts.

ment. An unknown offset to $Re(\epsilon'/\epsilon)$ has been added to the fitting procedure to mask out the central value for the systematic error study. Monte Carlo simulation was used to compare with various data distributions for the acceptance correction. Figure 7 and 8 show the good agreement of data/MC kaon decay z distribution comparison for both charged $\pi^+\pi^-$ and neutral $2\pi^0$ and $3\pi^0$ modes.

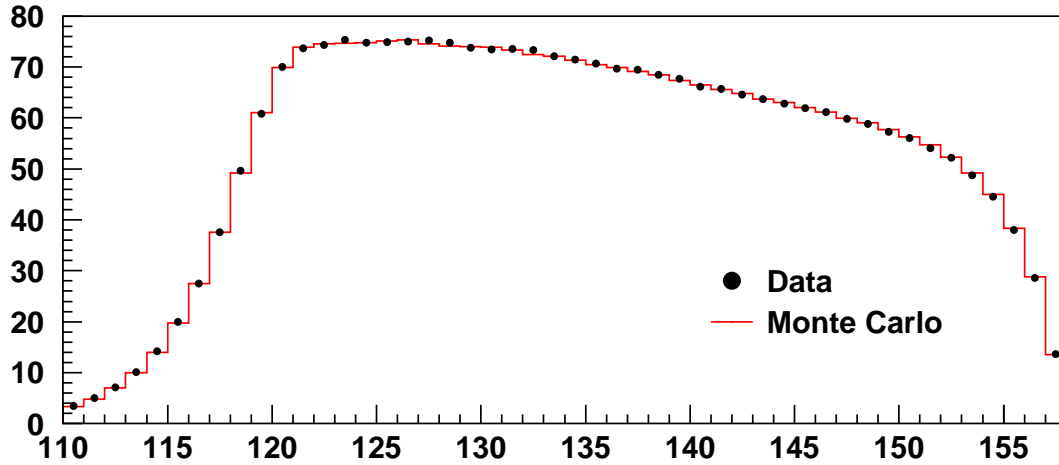
Systematic studies are currently in progress for the acceptance correction, detector calibration and energy scale, accidental effects, etc. with the use of high statistics $3\pi^0$, K_{e3} and $\pi^+\pi^-\pi^0$ samples as well as 2π decays. Improvements over E731 are expected, so the systematic error can be further reduced below 2.9×10^{-4} in $Re(\epsilon'/\epsilon)$.

4 Preliminary Results on $K_L \rightarrow \pi^0\gamma\gamma$

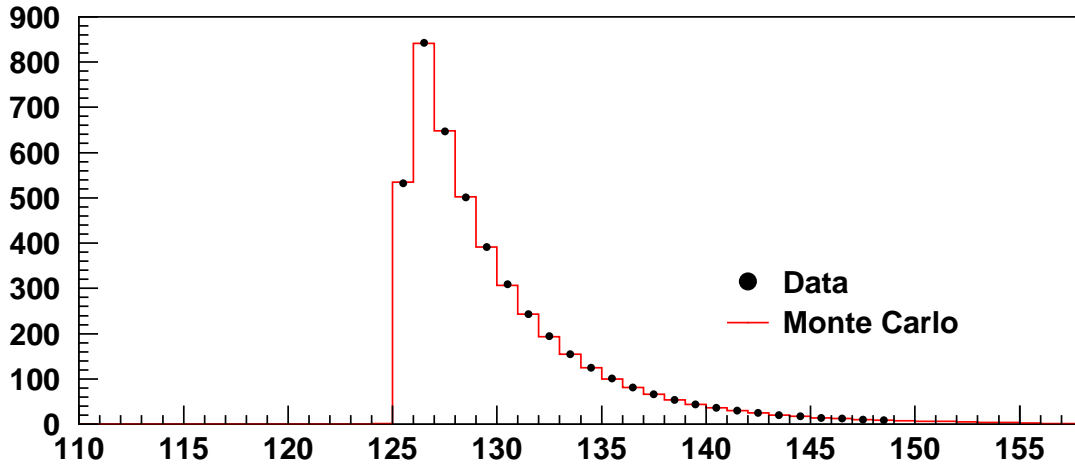
The decay $K_L \rightarrow \pi^0\gamma\gamma$ is of interest because it can be used to understand the contribution to the CP conserving amplitude for the rare decay $K_L \rightarrow \pi^0 e^+ e^-$, which is expected to have a large direct CP violating component. Because the $O(p^4)$ chiral perturbation $K_L \rightarrow \pi^0\gamma\gamma$ contributions to $K_L \rightarrow \pi^0 e^+ e^-$ are helicity suppressed, it was originally believed that the CP conserving amplitude for this decay would be negligible[12]. However, the vector meson exchange contribution to $K_L \rightarrow \pi^0\gamma\gamma$ have a different helicity structure than the $O(p^4)$ contributions and therefore can generate a large contribution to $K_L \rightarrow \pi^0 e^+ e^-$ that is many orders of magnitude larger than $O(p^4)$ amplitudes. Furthermore, the predicted $O(p^4)$ chiral calculation[13] for the branching ratio of $K_L \rightarrow \pi^0\gamma\gamma$ is almost three times smaller than the previous measurements[17][18] indicates the need for helicity allowed contributions[14][15]. Another new prediction from $O(p^6)$ calculation[16] is the presence of a low side tail in the $m_{\gamma\gamma}$ distribution, where the $\gamma\gamma$ refers to the two photons not associated with the π^0 . The previous experiments did not have enough sensitivity to see this tail. KTeV now has sufficient statistics to observe the possible low-side $m_{\gamma\gamma}$ tail and to compare with $O(p^6)$ chiral perturbation theory.

The $K_L \rightarrow \pi^0\gamma\gamma$ events were recorded at the same time with $2\pi^0$ decays in the ϵ'/ϵ data taking periods. The analysis requires two of the four photons be reconstructed within $3 \text{ MeV}/c^2$ of the nominal π^0 mass and the $m_{\gamma\gamma}$ from the other two photons be reconstructed $30 \text{ MeV}/c^2$ away from the π^0 mass. The π^0 mass resolution is $0.84 \text{ MeV}/c^2$. The dominant background is from $K_L \rightarrow \pi^0\pi^0\pi^0$ in which two of the six photons “fused” with other photons to appear as 4-photon-cluster event. To reduce such “fusion” background, we used the transverse photon shower shapes at the CsI calorimeter. Using simulated photon showers as a template, we have computed a “shape” χ^2 for each cluster using energies of the central 3×3 crystals in each cluster. The maximum shape χ^2 of the four cluster events is shown in Figure 9 for each $K_L \rightarrow \pi^0\gamma\gamma$ candidate. A peak is clearly seen at small value (below 3) of the shape χ^2 , and we interpret this peak as the $K_L \rightarrow \pi^0\gamma\gamma$ signal. The figure also shows the $3\pi^0$ background monte-carlo prediction for the tail in shape χ^2 . After applying a cut of shape $\chi^2 < 2.0$, a preliminary $m_{\gamma\gamma}$ distribution is shown in Figure 10(a). Figure 10(b) also shows the Dalitz variable y distribution, where $y = |E_3^* - E_4^*|/m_K$ and E_3^* and E_4^* are the energies of the two photons which are not associated with the π^0 in the kaon center of mass frame. There are 907 candidate

KTeV $K \rightarrow \pi^+\pi^-$ Data / MC Comparison (97a dataset)



$K \rightarrow \pi^+\pi^-$ vertex Z distribution, vacuum beam



$K \rightarrow \pi^+\pi^-$ vertex Z distribution, regenerator beam

Figure 7: Data and Monte-carlo comparison of the decay z distributions for (a) $K_L \rightarrow \pi^+\pi^-$ and (b) $K_S \rightarrow \pi^+\pi^-$ events, after all cuts.

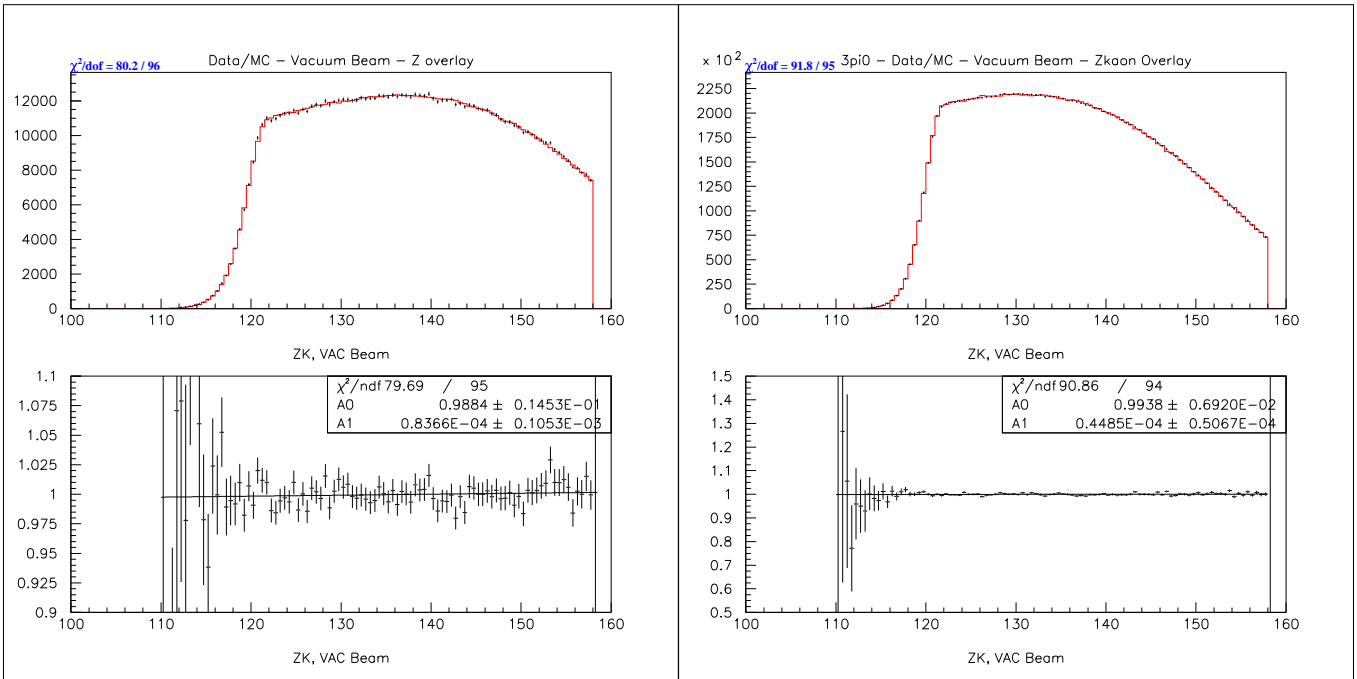


Figure 8: Data and Monte-carlo comparison of the decay z distributions for (a) $K_L \rightarrow \pi^0 \pi^0$ events after all cuts and the data/MC ratio, as well as (b) $K_L \rightarrow \pi^0 \pi^0 \pi^0$ events and the data/MC ratio.

events in which 796 events are signal and 111 ± 14 events are background. Normalizing this sample to $K_L \rightarrow \pi^0\pi^0$ (requiring $130 < m_{\gamma\gamma} < 140 \text{ MeV}/c^2$) gives a preliminary branching ratio of

$$BR(K_L \rightarrow \pi^0\gamma\gamma) = 1.76 \pm 0.06(stat) \pm 0.08(syst) \times 10^{-6}, \quad (4)$$

where the dominant systematic uncertainties are acceptance (2.4%), $3\pi^0$ background normalization (2.2%) and the uncertainty from $K_L \rightarrow \pi^0\pi^0$ branching ratio (2.1%) as well as the analysis cuts (3%). The acceptances are 3.13% for $K_L \rightarrow \pi^0\gamma\gamma$ and 3.23% for $\pi^0\pi^0$, respectively for events with energies between 40 and 160 GeV/c^2 and decaying in the region between 115 to 128 meters downstream from target.

The number of events with $m_{\gamma\gamma} < 240 \text{ MeV}/c^2$ is $83 \pm 14 \pm 9$, which is the first observation of the low-mass events for this decay mode. This corresponds to about 14% of the total decay rate after correcting for the events that are removed by the π^0 mass cut. The shape χ^2 distribution for these low-mass events is also shown in the inset of Figure 9, and clearly shows the signal peak. A fit to $m_{\gamma\gamma}$ and Dalitz variable y to extract the vector meson coupling gives, $a_V = -0.77 \pm 0.05 \pm 0.04$. This value of a_V corresponds to a CP conserving branching fraction for $K_L \rightarrow \pi^0 e^+ e^-$ between 1 to 2×10^{-12} which is 2 to 3 orders of magnitude higher than prediction based on the $O(p^4)$ calculations[13]. Our measured branching ratio agrees well with $O(p^6)$ calculation with $a_V = -0.77$, which gives 1.63×10^{-6} . The contribution of the direct CP violating amplitude to the rate for $K_L \rightarrow \pi^0 e^+ e^-$ is expected to be approximately 4×10^{-12} [19]. This suggests that the CP-conserving contribution to $K_L \rightarrow \pi^0 e^+ e^-$ will be comparable to the “direct” CP-violating one.

5 KTeV99

During the '96 and '97 fixed target run at Fermilab, KTeV has successfully accumulated large statistics sample for $\text{Re}(\epsilon'/\epsilon)$ measurement, as well as many other rare kaon decays[20][21]. The statistical uncertainty for $\text{Re}(\epsilon'/\epsilon)$ from the '96+'97 data sample is expected to be 1.5×10^{-4} . Further improvement in statistics will come from the upcoming 6-month '99 fixed target run. Based on the yield we had in '97 running period, we expect doubling the statistic sample for $\text{Re}(\epsilon'/\epsilon)$ in about 3-month smooth data taking period. Assuming that the systematic error on $\text{Re}(\epsilon'/\epsilon)$ of 10^{-4} or less will be achieved with higher statistics and better understanding of the detector performance, this may well be the most precise measurement in search for “direct” CP violation in the next 5 to 10 years before the next generation $K_L \rightarrow \pi^0\nu\bar{\nu}$ experiments. The rest data taking time in 1999 will be devoted to rare decay search program in kaon and hyperons, as well as continuing the study of $K_L \rightarrow \pi^0\nu\bar{\nu}$ in preparation for KAMI[22].

Several upgrades are currently in progress for the KTeV detector for the '99 run to improve both the performance and reliability of CsI calorimeter and drift chamber system. We are also improving the livetime for trigger and DAQ system to allow longer spill cycle and better duty factor (40 sec flat-top in 80 sec slow spill cycle at intensity of 10^{13} protons per spill) of the beam from the newly completed Main Injector and Tevatron at Fermilab.

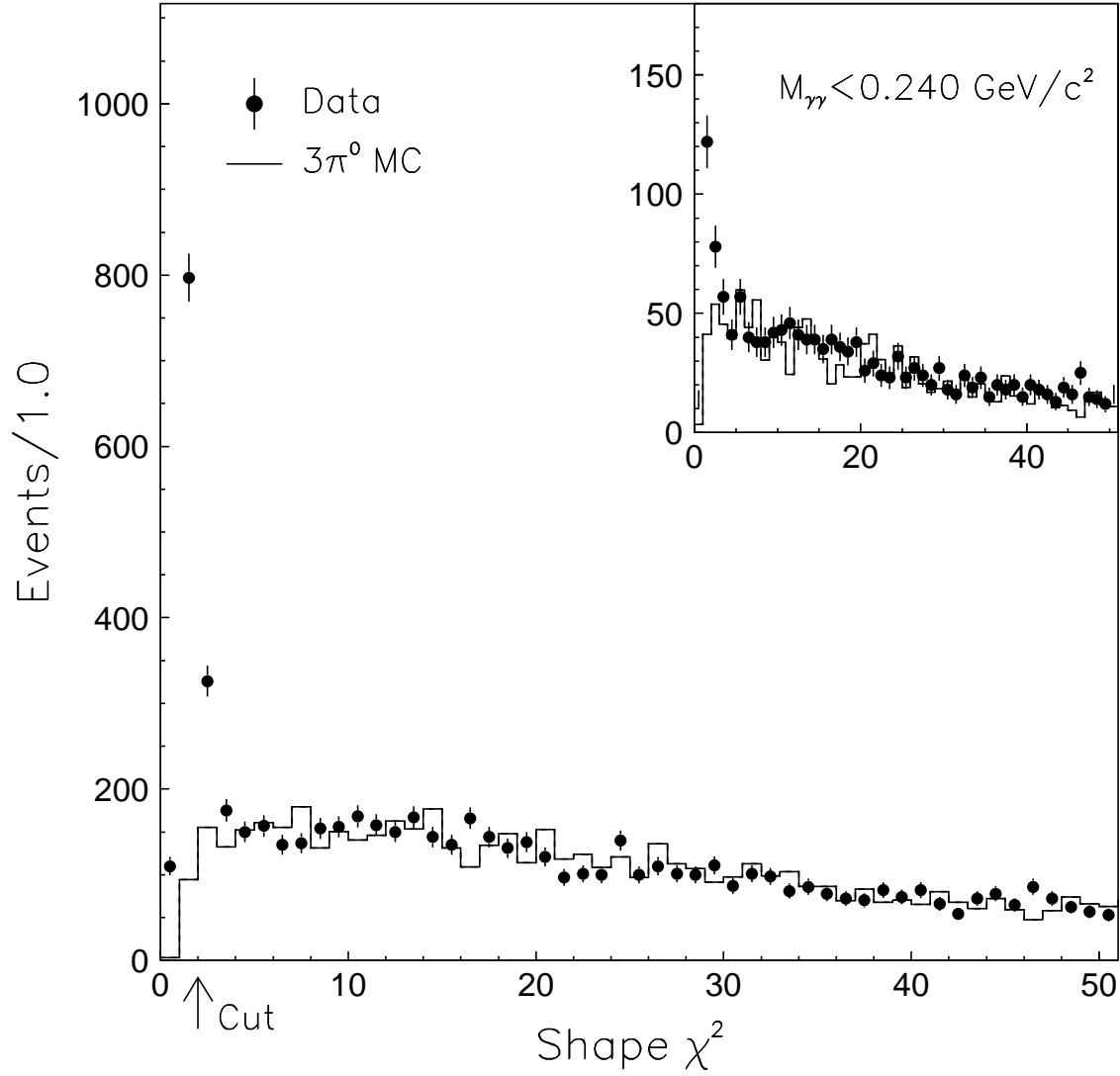


Figure 9: The maximum shape χ^2 of the four cluster $K_L \rightarrow \pi^0 \gamma \gamma$ candidates. The inset shows the same distribution for events with $m_{\gamma\gamma} < 240 \text{ MeV}/c^2$. The data are shown by dots; the histogram is from a Monte Carlo simulation of $K_L \rightarrow 3\pi^0$ events.

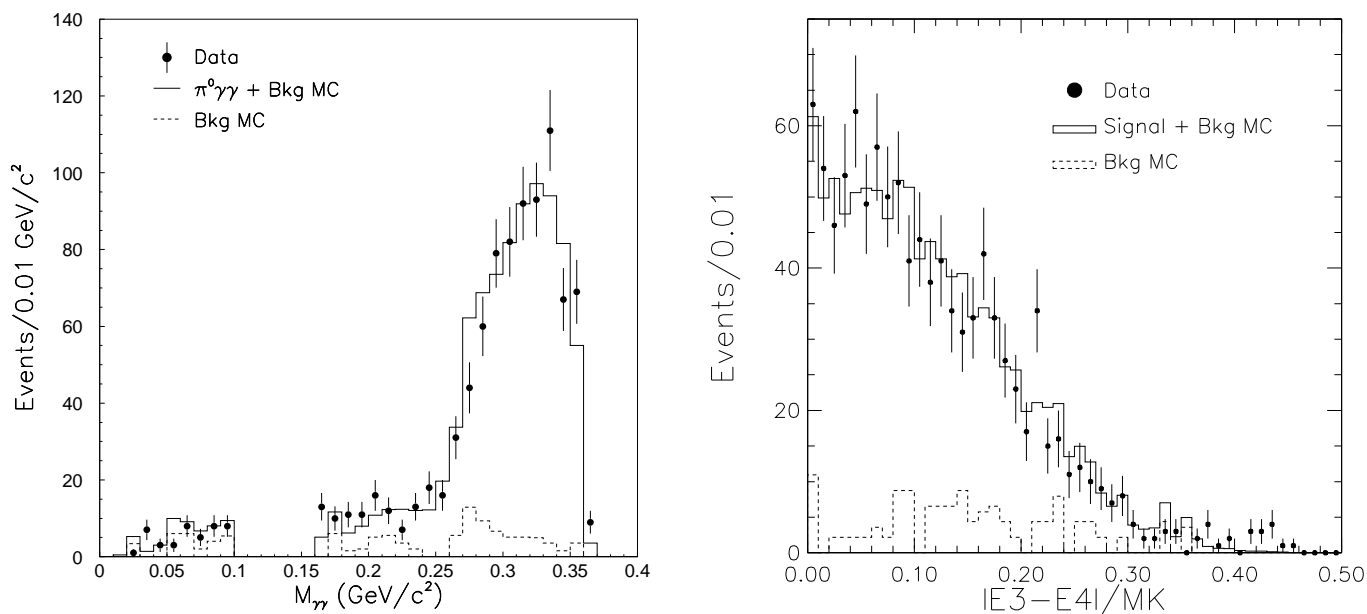


Figure 10: (a) The $m_{\gamma\gamma}$ distribution of the four cluster $K_L \rightarrow \pi^0\gamma\gamma$ candidates after shape $\chi^2 < 2.0$ cut. (b) The Dalitz y distribution for the $K_L \rightarrow \pi^0\gamma\gamma$ candidates. The data are shown by dots; the histogram is from a Monte Carlo simulation of $K_L \rightarrow \pi^0\gamma\gamma$ and $K_L \rightarrow 3\pi^0$ background events (dashed histogram).

References

- [1] B. Winstein and L. Wolfenstein, *Rev. Mod. Phys.* **65**, 1113 (1993).
- [2] L. K. Gibbons *et al.*, *Phys. Rev. Lett.* **70**, 1203 (1993); and *ibid.* *Phys. Rev.* **D55**, 6625, (1997).
- [3] G. D. Barr *et al.*, *Phys. Lett.* **B317**, 233 (1993).
- [4] J. M. Flynn and L. Randall, *Phys. Lett.* **B224**, 221 (1989); erratum *ibid.* *Phys. Lett.* **B235**, 412 (1990).
- [5] A. J. Buras, M. Jamin, M. E. Lautenbacher, *Phys. Lett.* **B389**, 749 (1996).
- [6] M. Ciuchini, E. Franco, G. Martinelli, L. Reina and L. Silvestrini, *Z. Phys.* **C68**, 239 (1995).
- [7] L. Wolfenstein, *Phys. Rev. Lett.* **13**, 569 (1964).
- [8] J. Cogan, “CERN NA48 ϵ'/ϵ ,” in the proceedings of this workshop.
- [9] F. Grancagnolo, “The Measurement of ϵ'/ϵ with KLOE at DAPHNE,” in the proceedings of this workshop.
- [10] G. Isidori, “Precision Tests and Search for New Physics with K Decays,” in the proceedings of this workshop.
- [11] A. J. Roodman, “The KTeV Pure CsI Calorimeter,” in Proceedings of the VII Intl. Conf. on Calorimetry (World Scientific, 1998).
- [12] G. Ecker, A. Pich and E. De Rafael, *Nucl. Phys.* **B303**, 665 (1988).
- [13] G. Ecker, A. Pich and E. De Rafael, *Phys. Lett.* **B189**, 363 (1987).
- [14] A. G. Cohen, G. Ecker and A. Pich, *Phys. Lett.* **B304**, 347 (1993).
- [15] P. Heiliger and L. M. Sehgal, *Phys. Rev.* **D47**, 4920 (1993).
- [16] G. D’Ambrosio and J. Portoles, *Nucl. Phys.* **B492**, 417 (1997).
- [17] G. D. Barr *et al.*, *Phys. Lett.* **B284**, 440 (1992).
- [18] V. Papadimitriou *et al.*, *Phys. Rev.* **D44**, 573 (1991).
- [19] J. F. Donoghue and F. Gabbiani, *Phys. Rev.* **D51**, 2187 (1995).
- [20] B. Cox, “KTeV E799 Rare Decays,” in the proceedings of this workshop.
- [21] K. Hanagaki, “KTeV $K_L \rightarrow \pi^0 \nu \bar{\nu}$ results,” in the proceedings of this workshop.
- [22] A. Barker, “ $K_L \rightarrow \pi^0 \nu \bar{\nu}$ at Fermilab (KAMI),” in the proceedings of this workshop.